High attenuation rate for shallow, small earthquakes in Japan

H. Si, K. Koketsu, H. Miyake & R. Ibrahim
Earthquake Research Institute, University of Tokyo, Japan

SUMMARY:
We compared attenuation characteristics of peak ground accelerations (PGAs) and velocities (PGVs) of the strong motion records from shallow, small earthquakes occurred in Japan with the ground motion prediction equation proposed by Si and Midorikawa (1999). From the comparison, we found that the observed PGAs and PGVs at stations far from the seismic source decay rapidly than those predicted by Si and Midorikawa (1999). The same tendencies are also reported in the past studies for deep, moderate and large earthquakes, but not for shallow, moderate and large earthquakes. In order to investigate the reason for the above results, we performed numerical simulations of strong ground motion for point sources of M_w 4 and 6, using a 2-D finite difference method and a standard earth structure proposed by Ueno et al. (2002) in Japan. Based on the analyses of the synthetic waveforms, we found that large surface waves were predominant only for moderate earthquakes and far stations. Generally the loss due to reflection on the boundaries in the discontinuous Earth's structure occur for all shallow earthquakes, but our results implicated that the loss is cancelled by surface waves for shallow, moderate and large earthquakes.

Keywords: Attenuation rate, PGA, PGV, Small earthquake, Moderate earthquake, Two-dimensional finite difference method

1. INTRODUCTION

Earthquake ground motions from small earthquakes are often used as empirical Green's functions in the prediction of strong motion from large earthquakes (e.g., Hartzell, 1978; Irikura, 1986; Dan and Sato, 1998), also used in the investigation of site effects and other important properties associated with strong ground motions at observation stations (e.g., Si et al., 2010, 2011). For a long time, however, since the strong motions from small earthquake are usually not associated with serious earthquake disasters, the attenuation characteristics of ground motion from small earthquakes have not been well investigated and understood. Recently, some of the research group associated with the NGA project have investigated the applicability of their models to the ground motions from small-to-moderate earthquakes, and found that the observations attenuate more rapidly than their NGA models (e.g., Atkinson and Morrison, 2009; Chiou et al., 2010; Campbell, 2011). In these studies, however, the physical background of the discrepancy between the observations and predictions are not clarified.

In this study, we focus on the attenuation characteristics of small earthquakes observed in Japan, and their differences with moderate or larger earthquakes. We try to make a physically based explanation for the discrepancy between small and moderate earthquakes based on a numerical simulation of seismic wave propagation.

2. ATTENUATION CHARACTERISTICS OF SMALL EARTHQUAKES

2.1. Data

We investigated the characteristics of attenuation for peak ground accelerations (PGAs) and velocities

(PGVs) from the small earthquakes with M_w around 4-5 occurred in Japan. In this paper, we show the results from six small earthquakes occurred in the Kanto area. Note that the same results also confirmed for the other areas in Japan. Table 2.1 shows the fundamental parameters and the information about the ground motion data from the six earthquakes used in this study. In the table, all the moment magnitudes were decided by NIED F-net.

For these earthquakes, the strong motion datasets recorded by K-NET operated by National Research Institute for Earth Science and Disaster Prevention (NIED) (Kinoshita, 1998) are used. The peak ground acceleration (PGA) is derived after filtering the seismic waves and the peak velocity (PGV) is derived by integrating the filtered acceleration waveform to velocity waveform. The peak values are defined as the larger one of two horizontal components. The soil profile of the observation stations are provided by NIED. The PGVs are corrected to rock site with a VS30 of 600 m/s based on the method proposed by Midorikawa et al. (1994). Hypocentral distances were accepted as the closest distances for the attenuation model, since for small earthquakes the two distances are thought to be almost the same. The range of the datasets is also described in Table 2.1.

Table 2.1. Earthquakes Used in the Study

Initial time (JST)	Location		M_w	Focal depth (km)	Number of data	Data range		
	Lat.	Long.				Distance (km)	PGA (cm/s^2)	PGV (cm/s, Vs=600 m/s)
2007/06/28 18:26	35.8	139.2	4.0	11.	61	14-150	0.8- 46.0	0.02-0.97
2007/07/12 05:29	35.5	139.1	3.9	20.	57	24-127	1.2- 94.5	0.02-1.75
2007/07/24 11:38	35.3	139.1	4.2	14.	86	21-147	1.0- 41.1	0.02-1.64
2007/08/18 04:14	35.4	140.4	4.9	20.	78	25-140	1.2-158.3	0.04-4.02
2007/10/01 02:21	35.2	139.1	4.7	11.	101	13-153	1.2-195.4	0.04-3.75
2009/02/17 04:54	35.3	140.3	4.5	20.	79	23-248	1.2- 34.2	0.02-1.01

2.2. Comparison of the observations with predictions

2.2.1. Ground motion prediction model

We compared the observed strong motion with the prediction by Si and Midorikawa (1999)(refer to SM1999 hereafter), shown in equations (2.1) and(2.2), which were developed based on the database derived in Japan, including earthquakes with a range of moment magnitudes covered from 5.8 to 8.3. In their models, PGA is defined on ground surface, while PGV is defined on bedrock with a shear wave velocity of about 600 m/s. The earthquakes are classified into three types, that is, crustal, inter-plate, and intra-plate earthquakes.

$$\log PGA=0.50M_w+0.0043D+d-\log(X+0.0055\cdot 10^{0.5Mw})-0.003X+0.61 \quad (2.1)$$

$$\log PGV=0.58M_w+0.0038D+d-\log(X+0.0028\cdot 10^{0.5Mw})-0.002X-1.29 \quad (2.2)$$

where X, M_w show fault distance, and moment magnitude, respectively. D is focal depth represented by the depth of the centre of a fault plane. d shows the coefficient for earthquake types, for PGA: 0.0 for crustal, 0.01 and 0.22 for inter- and intra-plate events; for PGV: 0.0 for crustal, -0.02 and 0.12 for inter- and intra-plate events, respectively.

These models have been checked with the earthquakes occurred in Japan after the models had been published, and the global data in the NGA database (e.g., Si et al., 2010). These infer that, generally the models represent the average attenuation rate for moderate and large shallow earthquakes.

2.2.2. Results

Figures 1 and 2 shows the comparison of observed PGAs and PGVs from the earthquakes listed in Table 2.1, with the predictions by Si and Midorikawa (1999). From the figures, though the observations generally match the predictions except for the records from event on 2007/08/18 04:14 for PGA and PGV, and event on 2007/08/18 04:14 for PGV, the attenuation rates, that is, the steepness of the decay in amplitude, are different. The records from small earthquakes seem attenuate rapidly than the predictions by SM1999. This phenomenon not only observed in the Kanto area, but also in other areas in Japan, and also reported for global earthquakes (e.g., Atkinson and Morrison, 2009; Chiou et al, 2010; Campbell, 2011). The same phenomenon are also reported for large deep earthquakes (e.g., Midorikawa and Ohtake, 2002; Nishimura and Horike, 2003).

Considering the reason of this phenomenon, for large deep earthquakes, Midorikawa and Ohtake (2002) suggested that, the steep attenuation rate may be caused by the reflection loss on the Mohorovicic discontinuity when focal depth deeper than about 30 km. This assumption may be valid for deep earthquakes, but cannot be applied to the shallow earthquakes since the focal depths generally located above the Mohorovicic discontinuity.

Here, we assume that the reflection loss proposed by Midorikawa and Ohtake (2002) occurred not only on significant discontinuity like the Mohorovicic discontinuity, but also on the boundaries for all the discontinuities in the Earth's structure. The assumption has been partially confirmed by Noda et al. (2011). Under this assumption, we can explain the steep attenuate rate for small shallow earthquakes, but cannot explain why the moderate and large shallow earthquakes attenuate in different way.

In order to investigate the difference between small and moderate shallow earthquakes in attenuation rates, we performed a numerical simulation for seismic wave propagation based on a two-dimensional finite difference method in the next chapter.

3. ATTENUATION OF SYNTHETIC MOTION FOR SMALL AND MODEREATE EARTHQUAKES

The numerical simulation for seismic wave propagation based on a two-dimensional finite difference method is described in this chapter. Based on the results, the attenuation characteristics of the synthetic peak values are discussed.

3.1. Method and model

A staggered 2D-FDM based on the method proposed by Graves (1996) is used for the simulation. In the method, absorbing boundary condition proposed by Clayton and Enquist (1977) and Cerjan et al. (1985) are used.

Simulation model is designed as a 300 km in horizontal direction (X axis) and 90 km in vertical direction (Z axis), divided by meshes with size of 0.1 km by 0.1 km. The velocity structure used in the simulation is the JMA2001 model proposed by Ueno et al. (2002), which is a standard model used to determine source location of the earthquakes occurred in Japan. Figure 3 shows the distribution of V_p and V_s of the JMA2001 model. V_{min} and V_{max} used in the calculation are 2.8 km/sec and 7.9 km/sec, relatively. The Q value is given as 10% of the wave-speed.

In the simulation, we calculated velocity waveforms for a double couple point source with a focal mechanism of strike = 179°, dip = 55°, rake = 82°, and a bell-shaped source time function $f(t) = [1 - \cos(2\pi t/T)]/T$, in which duration T are given in Table 3.1.

Scenario earthquakes with M_w of 4 and 6 are assigned as the target earthquake. Parameters include focal depths, duration of the source time functions are shown in Table 3.1.

Calculation are performed for 50,000 time-steps with a dt = 0.002 s, solving the wave equation with a F_{max} about 5 Hz. Synthetic seismic waves are calculated for 19 receivers located at distances ranged from 10 - 280 km.

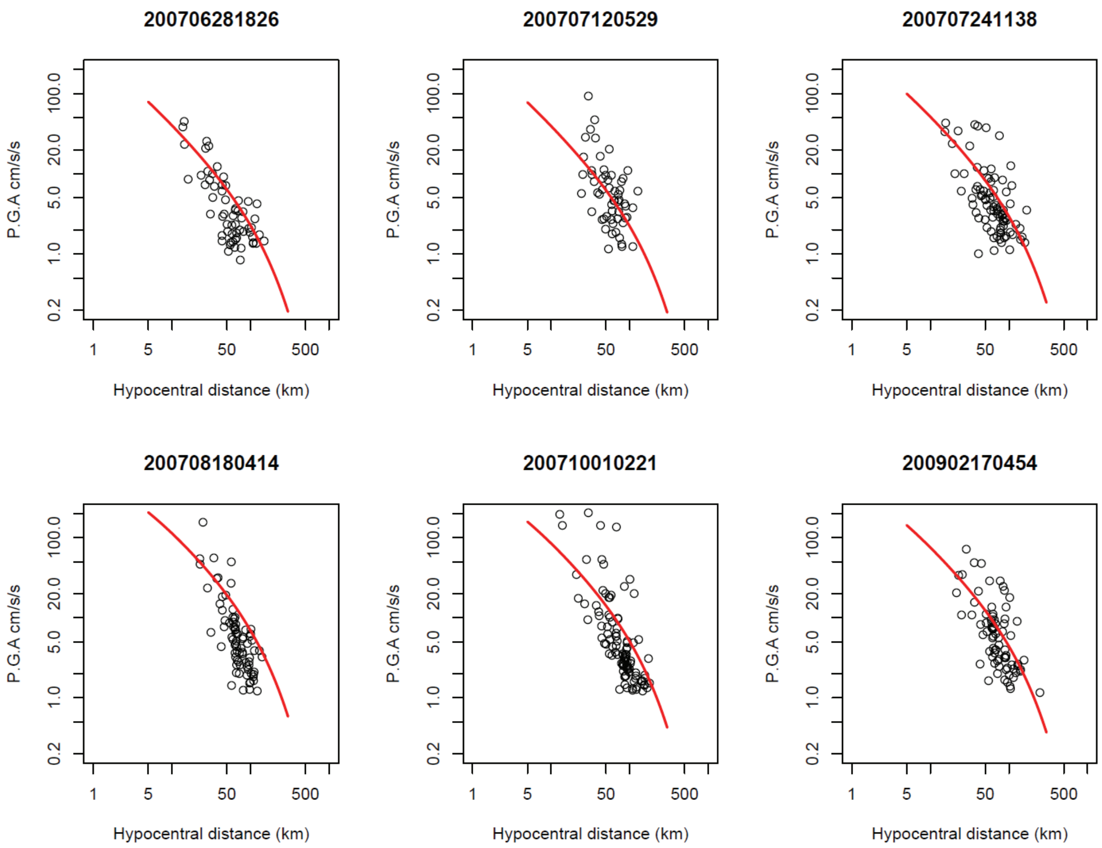

Figure 1. Comparison of observed PGAs and predictions by Si and Midorikawa (1999).

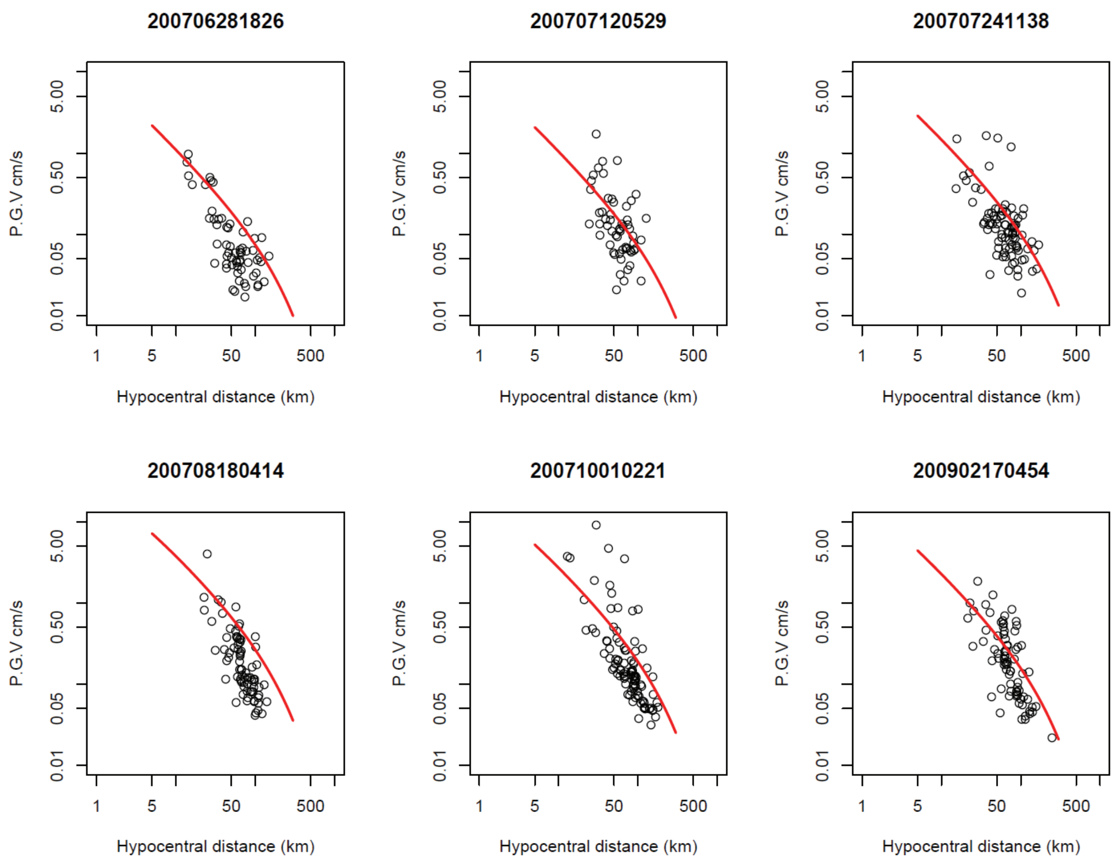

Figure 2. Comparison of observed PGVs and predictions by Si and Midorikawa (1999).

3.2. Results

Figure 4 shows the attenuation characteristics of PGAs and PGVs of synthetic waveforms for the four cases. Here, since the 2-D simulation assumes that the wave field and structure continue infinite in the direction perpendicular to the calculation model, so the amplitude of synthetic waveforms are generally relative values. For this reason, we normalized the amplitude both for waveforms and peak values. From the figure, the different attenuation rates are confirmed between the small and moderate earthquakes (both for focal depth of 10 and 20 km). The results are also consistent with the observations shown in Figure 1.

Figures 5 and 6 show the horizontal component of synthetic waveforms at each receiver for M_w=4 and 6, with a focal depth of 10 km, relatively. In the figures, distance is defined as hypocentral distance. It can be confirmed that the differences between the waveforms for M_w 4 and 6 is the performance of the Rayleigh waves. For the case of M_w=4, Rayleigh waves appeared clearly at receivers farther than 40 km. However, they become smaller and vanished from 110 km. For the case of M_w=6, Rayleigh waves keep predominant at receivers farther than 40 km.

Combining the results shown in Figures 4-6 and the results by Midorikawa and Ohtake (2002) and Noda et al. (2011), it can be indicated that (1) the attenuation rate for small earthquakes, $X^{-1.6}$, larger than those for body waves, may be caused by the reflection loss on the discontinuities in earth structure; (2) for moderate earthquakes, since the reflection loss almost be cancelled by the predominant surface waves (attenuation rate is $X^{-0.5}$), consequently, the attenuation rate shows the same as body waves ($X^{-1.0}$).

Table 3.1. Models for the Strong Motion Simulation

Model	M_w	Duration of the source time function	Focal depth (km)
Case 1-1	4.0	0.1 s	10.
Case 1-2			20.
Case 2-1	6.0	1.0 s	10.
Case 2-3			20.

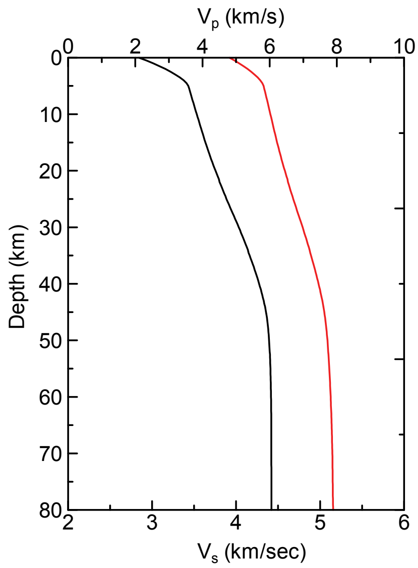

Figure 3. The JMA2001 model by Ueno et al. (2002) The black and red lines show V_p and V_s, relatively.

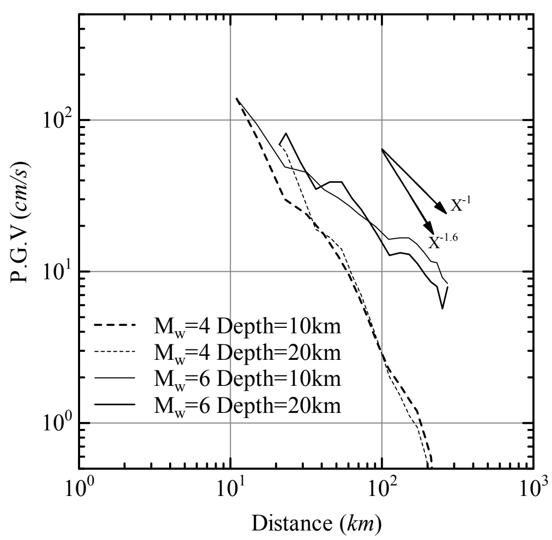

Figure 4. Differences in attenuation rate for synthetic results with different magnitudes and focal depths.

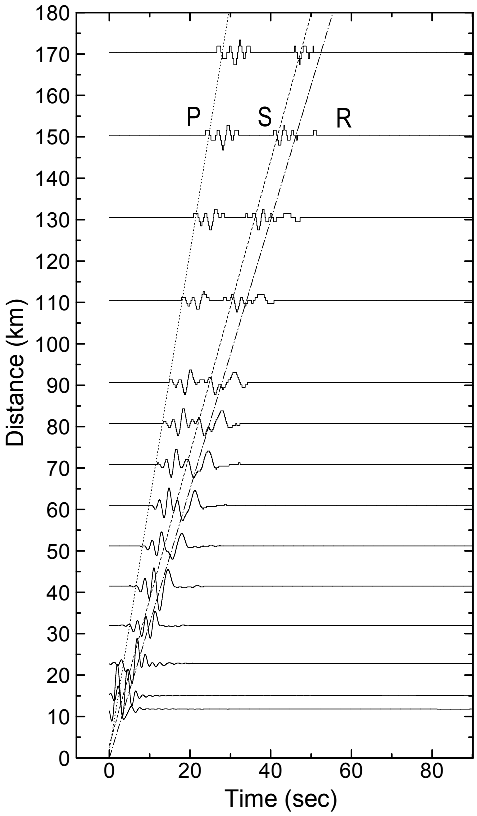

Figure 5. Synthetic seismic waves at receivers Lines show estimated onset time for P, S, and Rayleigh waves, relatively. (Case1-1, M_w=4)

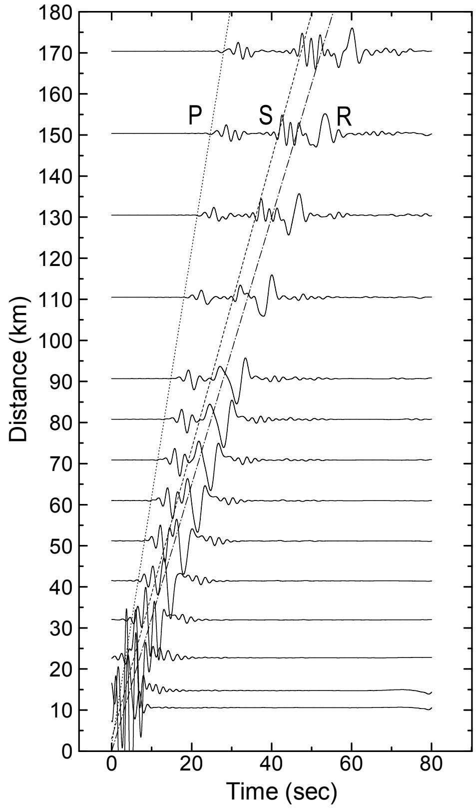

Figure 6. Synthetic seismic waves at receivers Lines show estimated onset time for P, S, and Rayleigh waves, relatively. (Case2-1, M_w=6)

4. DISCUSSION

In order to take the difference into account for the GMPEs, the method proposed by Midorikawa and Ohtake (2002) for representing the attenuation rate for deep earthquakes, are adopted. That is, for fault distances 1.7 times greater than the focal depth, instead of the term of log(X+C) in equation (1) and (2), the term of $(x+C))^{1.6}/(1.7D+C)^{0.6}$ are used. Where, $C=0.0055 \cdot 10^{0.5Mw}$ for PGA, and $0.0028 \cdot 10^{0.5Mw}$ for PGV. Comparison of this modified SM1999 and the observed PGAs and PGVs are shown in Figures 7 and 8. The figures show that the predictions are generally consistent with the observations, implying the validity of the results in this study.

5. CONCLUSION

In this study, we compared the attenuation characteristics of peak ground accelerations (PGAs) and velocities (PGVs) of the strong motion records from small earthquakes in Japan, and found that the observed PGAs and PGVs at far stations decay rapidly than those predicted by Si and Midorikawa (1999). In order to investigate the reason for the above results, we performed numerical simulations of strong ground motion for point sources of M_w 4 and 6, using a 2-D finite difference method. Based on the analyses of the synthetic waveforms, we found large surface waves were predominant only for moderate earthquakes and far stations. Generally the loss due to reflection on the boundaries in the discontinuous Earth's structure occur for all shallow earthquakes, but our results implied that the loss is cancelled by surface waves for shallow, moderate and large earthquakes.

AKCNOWLEDGEMENT

The strong motion data of K-NET were provided by National Research Institute for Earth Science and Disaster Prevention (NIED). This study is partially supported by the Research Funding for Earthquake Insurance in Japan operated by NLIRO and the Grants-in-Aid for Scientific Research "Construction of Next Generation of Ground Motion Prediction Equation (Project Number: 23241054, Principal Investigator: K. Koketsu)"

REFERENCES

Atkinson, G.M. and Morrison, M. (2009). Observations on Regional Variability in Ground-Motion Amplitudes for Small-to-Moderate Earthquakes in North America. *Bulletin of the Seismological Society of America.* **99:4**,2393-2409.

Cerjan, C., Kosloff, D., Kosloff, R. and Reshef, M. (1985). A nonreflecting boundary condition for discrete acoustic and elastic wave equations. *Geophysics.* **50**,705-708.

Chiou, K., Youngs, R., Abrahamson, N. and Addo, K. (2010). Ground-motion mttenuation model for small-to-moderate shallow crustal earthquakes in California and its implications on regionalization of ground-motion prediction models. *Earthquake Spectra.* **26:4**,907-926.

Clayton and Enquist (1977). Absorbing boundary conditions for acoustic and elastic wave equations. *Bulletin of the Seismological Society of America.* **67:6**,1529-1540.

Dan, K. and Sato, T. (1998). A semi-empirical method for simulating strong ground motions based on variable-slip rupture models for large earthquakes. *Bulletin of the Seismological Society of America.* **89:1**,36-53.

Graves, R.W. (1996). Simulating seismic wave propagation in 3D elastic media using staggered-grid finite differences. *Bulletin of the Seismological Society of America.* **86:4**,1091-1106.

Hartzell, S. (1978). Earthquake aftershocks as Green's functions. *Geophys. Res. Lett.* **5:1**,1-4.

Irikura, K. (1986). Prediction of strong acceleration motion using empirical Green's function. *Proceedings of the 7th Japan Earthquake Engineering Symposium.* 151-156.

Kinoshita, S. (1998). Kyoshin Net (K-NET). *Seismol. Res. Lett.* **69**, 309-332.

Midorikawa, S., Matsuoka, M. and Sakugawa, K. (1994). Site Effects on Strong-motion Records during the 1987 Chiba-ken-toho-oki, Japan Earthquake. *Proceedings of the 9th Japan Earthquake Engineering Symposium.* 85-90.

Midorikawa, S. and Ohtake, Y. (2002). Attenuation relationships of peak ground acceleration and velocity considering attenuation characteristics for shallow and deeper earthquakes. *Proceedings of the 11th Japan Earthquake Engineering Symposium.* 20-22 (in Japanese with English Abstract).

Nishimura, T. and Horike, M. (2003). The attenuation relationships of peak ground accelerations for the horizontal and the vertical components inferred from kyoshin network data. *J. Struct. Constr. Eng. AIJ.* **571**,63-70 (in Japanese with English Abstract).

Noda, A., Si, H. and Tokumitsu, R. (2011). Simulation study on the twofold spectral ratio using wavenumber integration method. *2011 Fall meeting of the Seismological Society of Japan.* C32-08 (in Japanese).

Si, H. and Midorikawa, S. (1999). New attenuation relationship for peak ground acceleration and velocity considering effects of fault type and site condition. *J. Struct. Constr. Eng. AIJ.* **523**,63-70 (in Japanese with English Caption and Abstract).

Si, H., Tsutsumi, H. and Midorikawa, S. (2010). Evaluation of Hanging Wall Effects on Ground Motion Attenuation Relationship Correcting the Site effects. *Proceedings of the 9thNCEE/10CCEE.* Paper No.467.

Si, H., Kuyuk, H.S., Koketsu, K., Miyake, H. and Ibrahim, R. (2011). Estimation of Site Effects based on Recorded Data and the Ground Motion Attenuation Relationship. *4th IASPEI / IAEE International Symposium: Effects of Surface Geology on Seismic Motion. Paper No.6.7.*

Ueno, H., Hatakeyama, S., Aketagawa, T., Funasaki, J. and Hamada, N. (2002). Improvement of hypocenter determination procedures in the Japan Meteorological Agency. *Quarterly Journal of Seismology*, **65**,123-134.

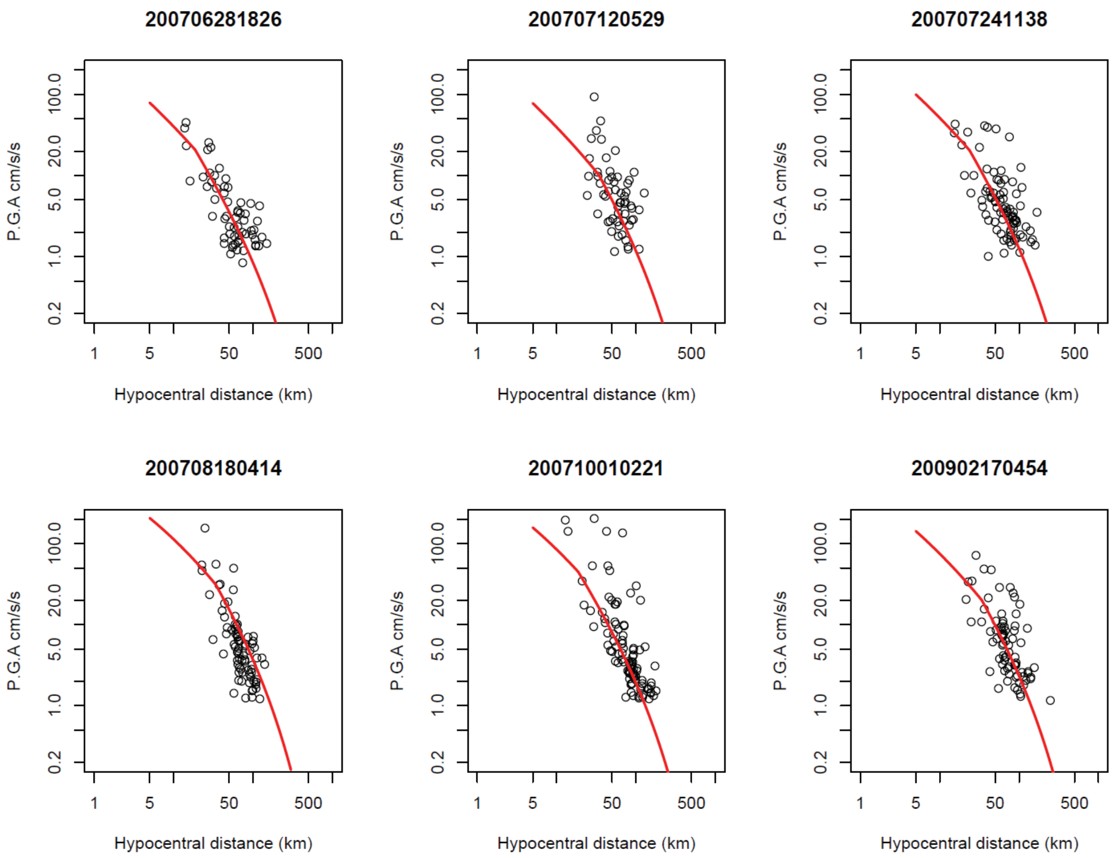

Figure 7. Comparison of observed PGAs and predictions by SM1999 modified for attenuation rate.

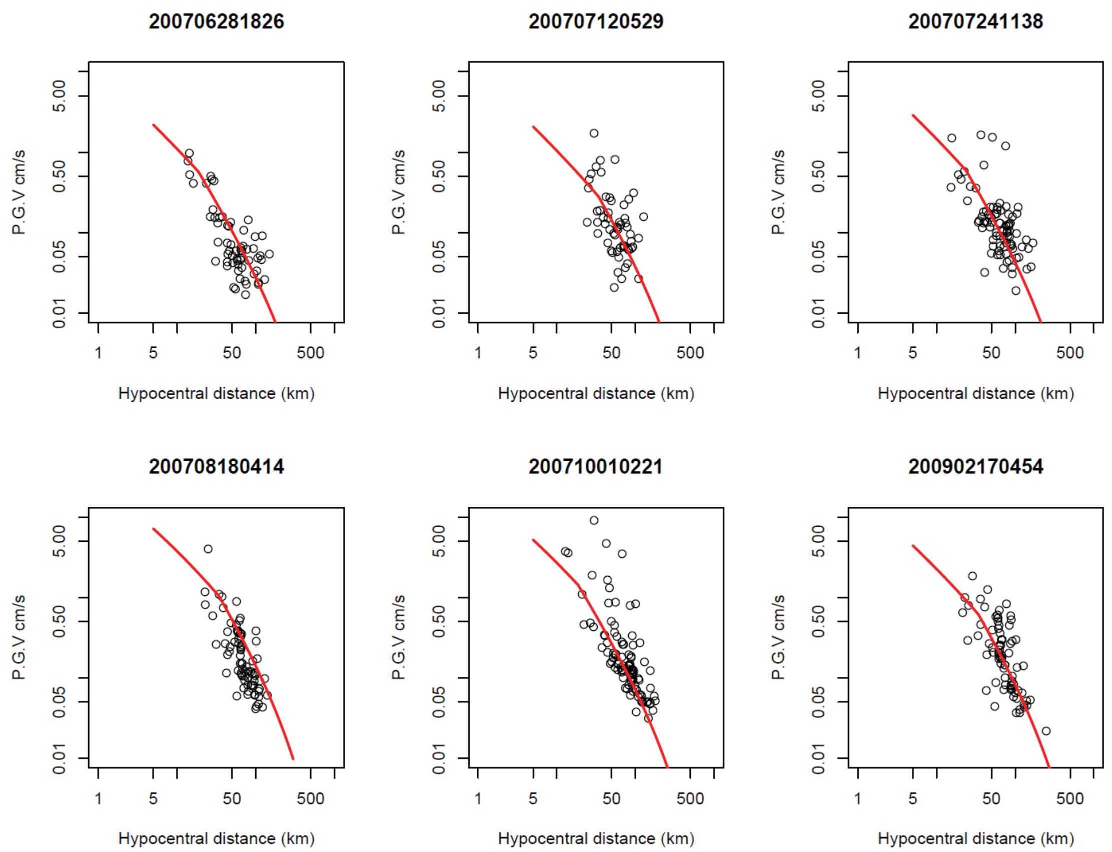

Figure 8. Comparison of observed PGVs and predictions by SM1999 modified for attenuation rate.